An Induced-Fit Kinetic Mechanism for DNA Replication Fidelity: Direct Measurement by Single-Turnover Kinetics[†]

Isaac Wong, Smita S. Patel, and Kenneth A. Johnson*

Department of Molecular and Cell Biology, 301 Althouse Laboratory, The Pennsylvania State University, University Park, Pennsylvania 16802

Received February 5, 1990; Revised Manuscript Received August 16, 1990

ABSTRACT: An exonuclease-deficient mutant of T7 DNA polymerase was constructed and utilized in a series of kinetic studies on misincorporation and next correct dNTP incorporation. By using a synthetic oligonucleotide template–primer system for which the kinetic pathway for correct incorporation has been solved [Patel, S. S., Wong, I., & Johnson, K. A. (1991) *Biochemistry* (first of three papers in this issue)], the kinetic parameters for the incorporation of the incorrect triphosphates dATP, dCTP, and dGTP were determined, giving, respectively, k_{cat}/K_m values of 91, 23, and 4.3 M^{-1} s^{-1} and a discrimination in the polymerization step of 10^5–10^6. The rates of misincorporation in all cases were linearly dependent on substrate concentration up to 4 mM, beyond which severe inhibition was observed. Competition of correct incorporation versus dCTP revealed an estimated K_i of ~6–8 mM, suggesting a corresponding k_{cat} of 0.14 s^{-1}. Moderate elemental effects of 19-, 17-, and 34-fold reduction in rates were measured by substituting the α-thiotriphosphate analogues for dATP, dCTP, and dGTP, respectively, indicating that the chemistry step is partially rate-limiting. The absence of a burst of incorporation during the first turnover places the rate-limiting step at a triphosphate binding induced conformational change before chemistry. In contrast, the incorporation of the next correct triphosphate, dCTP, on a mismatched DNA substrate was saturable with a K_m of 87 μM for dCTP, 4-fold higher than the K_d for the correct incorporation on duplex DNA, and a k_{cat} of 0.025 s^{-1}. A larger elemental effect of 60, however, suggests a rate-limiting chemistry step. The rate of pyrophosphorolysis on a mismatched 3'-end is undetectable, indicating that pyrophosphorolysis does not play a proofreading role in replication. These results show convincingly that the T7 DNA polymerase discriminates against the incorrect triphosphate by an induced-fit conformational change and that, following misincorporation, the enzyme then selects against the resultant mismatched DNA by a slow, rate-limiting chemistry step, thereby allowing sufficient time for the release of the mismatched DNA from the polymerase active site to be followed by exonucleolytic error correction.

Models to explain the high fidelity of DNA replication have long been proposed in the literature [reviewed in Loeb and Kunkel (1982)]. For example, several models have invoked a role for pyrophosphorolysis in fidelity by mechanisms sometimes referred to as "kinetic proofreading" (Brutlag & Kornberg, 1972; Deutscher & Kornberg, 1969; Hopfield, 1976; Ninio, 1975). It is, however, worth noting that the original models have been proposed as purely mathematical constructs, and the only evidence in support of a role for pyrophosphorolysis is the observation that polymerization is less accurate at high pyrophosphate concentrations (Kunkel et al., 1986). Although induced-fit mechanisms have been suggested, it has also been argued that induced-fit models cannot account for increased selectivity (Fersht, 1974, 1985; Page, 1986). Thus, because of a void of mechanistic information, almost all of these models take considerable liberties with invoking specific but unsubstantiated intermediates in the kinetic pathway of polymerization. Furthermore, most of the published mechanistic studies available on misincorporation rely solely on steady-state kinetic data, which, as we will show, are at best difficult to interpret and at worst extremely misleading. The only transient kinetic study on the mechanism of DNA polymerization relied upon the use of the Klenow fragment of the DNA repair enzyme, Pol I, and some surprising results were obtained, the most notable of which is that the polymerase

Scheme I
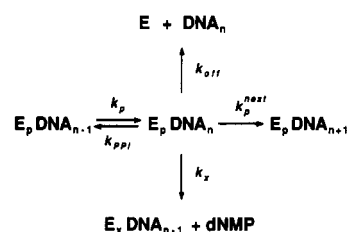
bound correct and incorrect dNTPs with nearly equal affinities (Kuchta et al., 1987, 1988).

In this report, we propose a mechanism for DNA replication fidelity as a part of our kinetic study of the T7 DNA polymerase (Patel et al., 1991; Donlin et al., 1991). The T7 system lends itself especially well to our approach to fidelity because its kinetic scheme has been completely solved (Patel et al., 1991; Donlin et al., 1991). Consequently, our results can be interpreted by a direct comparison of the differences between correct and incorrect polymerization. In general, T7 DNA polymerase constitutes a nearly ideal model system for any DNA replication studies because it functions in vivo as a true replication enzyme with a minimal number of components.

The problem of replication fidelity is summarized in Scheme I. Conceptually, we divide the issue of fidelity into two parts. First, we are concerned with the mechanism of making an error; this primarily involves solving the kinetics of misincorporation. Second, we are interested in the kinetic consequences of the error; here, we must determine the relative

*To whom correspondence should be addressed.

Table I: Oligonucleotides

25/36-mer	5'-GCCTCGCAGCCGTCCAACCAACTCA CGGAGCGTCGGCAGGTTGGTTGAGTAGGTCTTGTTT-5'
25A/36-mer	5'-GCCTCGCAGCCGTCCAACCAACTCA^A CGGAGCGTCGGCAGGTTGGTTGAGTAGGTCTTGTTT-5'

contribution—the kinetic partitioning—between the four possible exit pathways from the central "enzyme–error" complex: (1) pyrophosphorolysis, which represents the microscopic reversal of polymerization, (2) incorporation of the next correct dNTP, (3) dissociation of the mismatched DNA from the enzyme into free solution, and (4) direct transfer of the mismatched DNA into the exonuclease site for repair.

Paradoxically, the chief disadvantage of the T7 system lies in its high replication fidelity. Wild-type enzyme does not form detectable levels of stable misincorporations in vitro. This, as we will show, is due to the highly efficient 3'–5' proofreading exonuclease, which is particularly good at excising mismatches. For this reason, we have constructed an exonuclease-deficient mutant enzyme (D5A,E7A) (Patel et al., 1991) on the basis of sequence homology studies (Reha-Krantz, 1988a,b; Leavitt & Ito, 1989; Bernad et al., 1989). Using this mutant polymerase, we are able to study the kinetic mechanism and consequences of misincorporation. On the basis of these studies, we propose here that, in a normal cycle of polymerization involving correct incorporation, a rate-limiting conformational change step in an induced-fit mechanism bears the primary burden of substrate selectivity. The issues of (1) V_{max} versus K_m discrimination in substrate selectivity, (2) the role of pyrophosphorolysis in error correction, and (3) the kinetic partitioning mechanism for exonucleolytic error repair will all be discussed in the context of this induced-fit model.

EXPERIMENTAL PROCEDURES

Materials

Bacterial Strains, Plasmids, and Phage. *Escherichia coli* A179 (Hfr-C)(λ)*trxA::kan*) and plasmids of pGP5-3 and pGP1-3 were obtained from S. Tabor and C. C. Richardson (Harvard Medical School; Tabor & Richardson, 1987). The plasmid containing the exo⁻ T7 gene 5, pGA1-14, was constructed in this laboratory as described in the preceding paper (Patel et al., 1991).

Proteins and Enzymes. *E. coli* thioredoxin was purified as described in the preceding paper. Klenow fragment (KF) was kindly provided by R. Kuchta and C. Catalano (The Pennsylvania State University). T4 polynucleotide kinase was purchased from New England Biolabs.

Nucleoside Triphosphates. dNTPs were purchased from Pharmacia Molecular Biologicals at >98% purity. ATP was purchased from Sigma. [α-^{32}P]dTTP, [α-^{32}P]dCTP, [α-^{32}P]dATP, and [γ-^{32}P]ATP were purchased from New England Nuclear.

Synthetic Oligonucleotides. Synthetic oligonucleotides (see Table I) used were synthesized on either an Applied Biosystems 380A DNA synthesizer or a Milligen/Biosearch 7500 DNA synthesizer and purified by electrophoresis through a denaturing gel (20% acrylamide, 1.5% bisacrylamide, and 8M urea in Tris–borate buffer). The major DNA band was visualized by UV shadowing and excised. DNA was electroeluted from the gel slice in an Elutrap apparatus purchased from Schleicher & Schuell. Triethylammonium bicarbonate (TEAB; 2 M, pH 7.5) was added to a final concentration of 0.5 M, and the eluate was applied to an Alltech Maxi-Clean C$_{18}$ cartridge. After being washed with 10 mM TEAB, pH

7.5, purified DNA was eluted in 50% ethanol. Concentrations of purified oligonucleotides were determined by UV absorbance at 260 nm in 8 M urea the following extinction calculated coefficients: 20-mer, ε = 202 450; 25-mer, ε = 249 040; 25A-mer, ε = 261 040; 36-mer, ε = 377 000 cm²/μmol.

Duplex Oligonucleotides. Duplex oligonucleotides were annealed at room temperature in TE buffer containing 100 mM NaCl. They were then purified by electrophoresis through a nondenaturing gel (20% acrylamide and 1.5% bisacrylamide in Tris–borate buffer). The major DNA band was visualized, excised, and electroeluted as above.

Methods

25A/36-mer. Template–primer containing a 3'-terminal A-A mismatch was enzymatically synthesized by using exo⁻ T7 DNA polymerase. The 25/36-mer (1 μM) was incubated with enzyme (500 nM) and dATP (2 mM) for 5 min at room temperature. Reaction was quenched by the addition of EDTA to 50 mM, followed by two extractions with buffer-saturated phenol–chloroform (1:1). Unincorporated dATP and EDTA as well as residual phenol–chloroform were removed by centrifugation through Bio-Spin 30 centrifuge desalting columns.

3'-^{32}P-Labeled 25A/36-mer. The 25/36-mer (1 μM) was incubated with enzyme (500 nM) and [α-^{32}P]dATP (3000 Ci/mmol at a final concentration of 2–3 μM) for 45 min at room temperature. Cold dATP (2 mM) and an additional aliquot of enzyme (250 nM) were added, and incubation was continued for an additional 5 min. Workup of labeled DNA was as described above.

Reaction Buffer, 5' ^{32}P Labeling, Reconstitution of T7 DNA Polymerase, Rapid-Quench Experiments, Product Analysis by Denaturing Acrylamide Gels, and PEI-Cellulose TLC. These protocols were performed exactly as described in detail in the first paper in this series (Patel et al., 1991).

RESULTS

Determination of K_m and k_{cat} for Incorporation of the Incorrect dNTPs. We began our studies by attempting to determine the steady-state kinetic parameters, K_m and k_{cat}, for incorrect dNTP incorporation. The DNA substrate used was a 5'-labeled 25/36-mer, and the time courses of incorporation were monitored by analysis of the products on denaturing sequencing gels. The misincorporation of dATP and dGTP (versus A in the template) led to elongation of the 25-mer by one base, while the misincorporation of dCTP led to a series of four bands of sizes 26–29 bases. This resulted from the fact that, after the initial misincorporation to generate the 26-mer, dCTP was the correct base for the next two additions (27- and 28-mers); at higher concentrations of dCTP and at longer time points, a second misincorporation on the 28-mer generated the 29-mer. All four bands were excised, counted, and summed to yield the total products, thus defining the kinetics of the first misincorporation.

The rates of misincorporation for the three incorrect dNTPs were determined over a range of dNTP concentrations from 5 μM up to 10 mM. The results in the millimolar range are shown in Figure 1A. Misincorporation rates were found to be linearly dependent on dNTP concentrations up to 4 mM. Beyond 4 mM, severe inhibition was observed, presumably due to inhibition of DNA binding. Regression analysis gave linear best fits to the data with the slopes defining the apparent second-order rate constant, k_{cat}/K_m. The k_{cat}/K_m values for dATP, dCTP, and dGTP were 91, 23, and 4.3 M⁻¹ s⁻¹, respectively. Although there was no indication of curvature in the data prior to the onset of the severe inhibition, we can
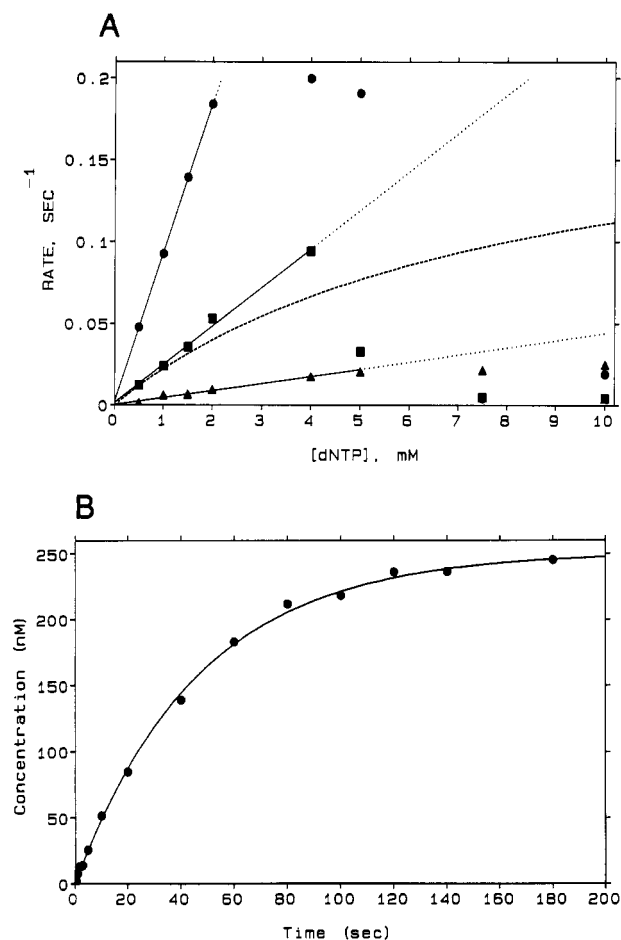
FIGURE 1: Misincorporations. Panel A shows a plot of rates of misincorporation onto 25/36-mer as a function of dNTP concentration. The slopes of the solid lines yield the values of k_{cat}/K_m: (▲) dGTP, $k_{cat}/K_m = 4.2$ M^{-1} s^{-1}; (■) dCTP, $k_{cat}/K_m = 23$ M^{-1} s^{-1}; (●) dATP, $k_{cat}/K_m = 91$ M^{-1} s^{-1}. The concentration dependence continues to be linear until 4 mM, beyond which the rate of misincorporation is severely inhibited. The dashed line shows an attempted hyperbolic fit to estimated lower limits for K_m of 8 mM and a k_{cat} of 0.2 s^{-1} for the dCTP data with a resultant k_{cat}/K_m of 25 M^{-1} s^{-1}. Reactions were all carried out under steady-state conditions with 1 μM 25/36-mer and 5 nM enzyme. Reactions were quenched by the addition of EDTA to 125 mM, and the products were analyzed by denaturing sequencing gels. Quantitation of products was by excision and liquid scintillation counting of gel bands. Panel B shows the time course of a single-turnover dCTP misincorporation at 250 nM enzyme, 250 nM DNA, and 1 mM dCTP. The best fit of the data to a single exponential yields a rate of 0.021 s^{-1}, indicating that the rate during the first turnover is the same as the steady-state rate.

estimate the K_m on the basis of data describing the inhibition of correct incorporation by the incorrect dCTP (see below). The dashed line in Figure 1A represents the calculated hyperbola for a K_m of 8 mM at a k_{cat} of 0.2 s^{-1} ($k_{cat}/K_m = 25$ M^{-1} s^{-1}), setting a lower limit on the magnitudes of K_m and k_{cat}.

While these experiments were carried out under steady-state conditions in which DNA was in 200-fold excess over enzyme, an experiment performed under pre-steady-state conditions, with a 1:1 ratio of DNA to enzyme, indicated that the rate during the first turnover was the same as that for subsequent turnovers (Figure 1B). Even given the subsaturating concentration of dNTP used in the single-turnover experiments, biphasic kinetics would have been expected if the steady-state rate measured some rate-limiting step after chemistry, given a detection limit of 5%. Consequently, within this limit, we conclude that the steady-state rates reported in Figure 1 reflect the rate of misincorporation and not the rate of product
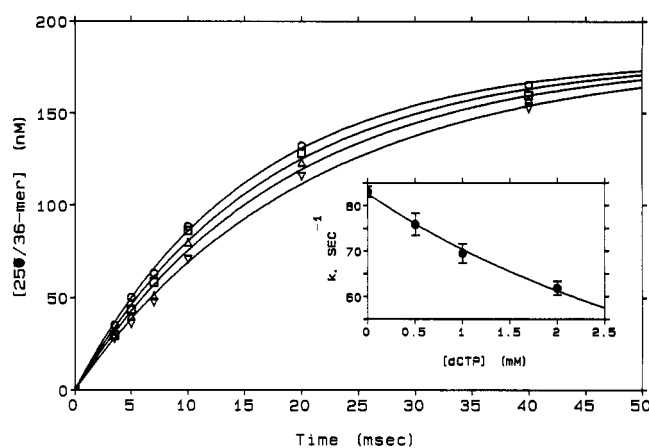

FIGURE 2: Inhibition of correct incorporation by incorrect dNTP. Time course of correct incorporation at 10 μM dTTP in the presence of 0 (O), 0.5 (□), 1.0 (△), and 2.0 mM (▽) of the incorrect dCTP. Solid curves are best fits of the data to single exponentials with rates of 83, 76, 69, and 62 s^{-1}, respectively. Inset shows rate of correct incorporation as a function of dCTP concentration fitted to a hyperbola to yield an extrapolated K_i for dCTP of 4 ± 2 mM. Enzyme and DNA concentrations were 250 nM each. The degree of inhibition observed is so small that the error on the K_i is correspondingly large. Taken together with the estimated lower limit of 8 mM observed in the experiment described in Figure 1, we would estimate a reasonable range for the K_m of dCTP to be around 6–8 mM. See text for further descriptions on the practical constraints in designing these experiments.

(DNA) dissociation, as is the case for correct incorporation.

In a separate attempt to extract discrete values of k_{cat} and K_m for misincorporation, a competition experiment was performed to determine a K_i for inhibition of correct incorporation (dTTP) by an incorrect dNTP (dCTP). DNA (5'-labeled 25/36-mer at 250 nM) was preincubated with 250 nM exo$^-$ enzyme and then was reacted with 10 μM Mg·dTTP (correct dNTP) to measure the rate of the burst of correct incorporation in the presence of 0, 0.5, 1, and 2 mM dCTP (Figure 2). From the concentration dependence of the effect of the incorrect dNTP on the rate of correct incorporation, a K_i for the incorrect dNTP can be very roughly estimated at 4 ± 2 mM. However, the overall degree of inhibition observed was slight, and therefore, the value of K_i thus derived was heavily extrapolated. Taken together with the limit of 8 mM estimated in Figure 1A (see above description), we estimate an approximate range for K_m of 6–8 mM to be within reasonable limits of experimental errors. Unfortunately, the severe inhibition observed at higher dNTP concentrations precluded a better measurement of the K_m for misincorporation.

Elemental Effect for Misincorporation. In order to estimate the extent to which the chemistry step is rate-limiting, we compared the rates of misincorporations of dATP, dCTP, and dGTP with their α-thio analogues dATP(αS), dCTP(αS), and dGTP(αS). A full elemental effect, resulting in a 100-fold reduction of rate when the thio analogues are substituted for the oxy-dNTPs, would indicate a completely rate-limiting chemistry step. For the incorporation of the correct nucleoside triphosphate, dTTP, a small elemental effect of 3 has been observed (Patel et al., 1991), indicating that the chemistry step is not rate-limiting during a normal cycle of polymerization.

In these experiments, 5'-labeled 25/36-mer was used at a 5-fold molar excess over enzyme. Data were quantitated by excision and liquid scintillation counting of bands from a denaturing sequencing gel. The time courses of incorporation of the oxy-dNTPs and the α-thio-dNTPs are shown in Figure 3. Substitution by the thio analogues resulted in reduction in incorporation rates by factors of 19, 17, and 37 for dATP, dCTP, and dGTP, respectively. These moderate values may
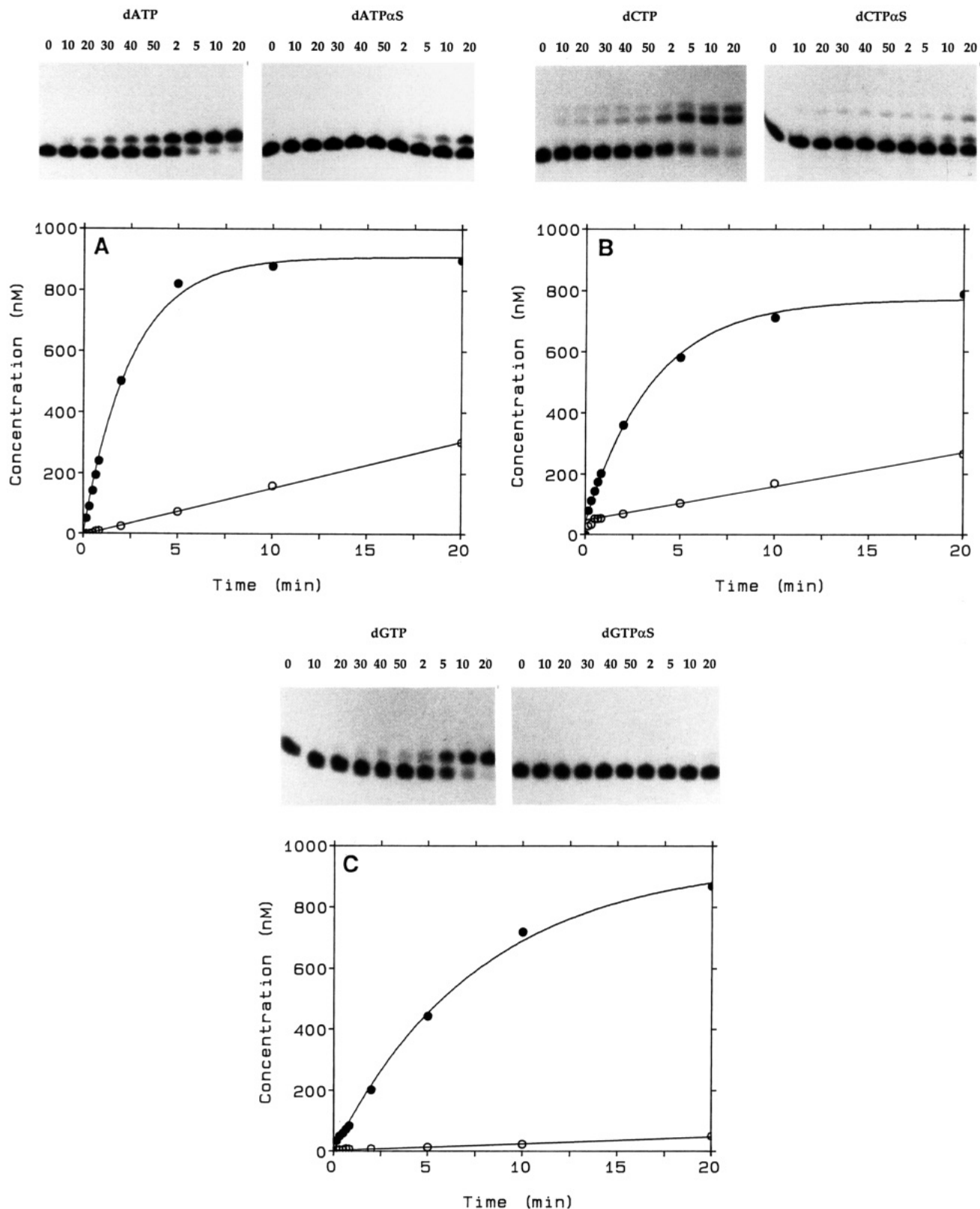
FIGURE 3: Elemental effects on misincorporations. Time course of misincorporation of dATP, dCTP, and dGTP (●) and their α-thio analogues dATP(αS), dCTP(αS), and dGTP(αS) (O). Panel A shows dATP and dATP(αS) misincorporations at 2.4×10^{-2} and 1.3×10^{-3} s^{-1}, respectively. Panel B shows dCTP and dCTP(αS) misincorporations at 1.6×10^{-2} and 9.3×10^{-4} s^{-1}, respectively. As noted in the text, because dCTP is the correct triphosphate for the next two incorporations, a ladder of products from 26 to 29 bases was observed. The difference in banding patterns between the dCTP and dCTP(αS) lanes is illustrative of the difference in elemental effects on dCTP misincorporation and next correct incorporation. With dCTP, the incorporation of the correct dCTPs after the misincorporation is faster than misincorporation and therefore no net accumulation of the 25C-mer is observed. However, because the elemental effect on misincorporation of dCTP is smaller than that for the next correct incorporation, the rate of addition of the next dCTP(αS) in the correctly base-paired positions is now actually slower than the rate of misincorporation, resulting in the accumulation of the 25C-mer. Panel C shows dGTP and dGTP(αS) misincorporations at 7.1×10^{-3} and 1.9×10^{-4} s^{-1}, respectively. Overall elemental effects for dATP, dCTP, and dGTP are 19, 17, and 37. Reaction incubations contained 1 μM 25/36-mer, 200 nM enzyme, and 250 μM, 750 μM, and 1.5 mM dATP, dCTP, and dGTP, respectively, in standard reaction buffer.
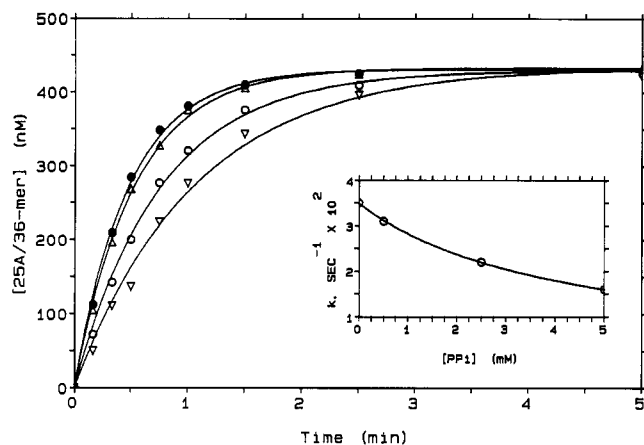
FIGURE 4: Inhibition of misincorporation by pyrophosphate. The rates of misincorporation of dATP (500 μM) into 25/36-mer (500 nM) at 500 nM enzyme at 0 ($\bullet$), 0.5 ($\triangle$), 2.5 ($\bigcirc$), and 5.0 mM ($\triangledown$) pyrophosphate. Inset shows the plot of the rates fitted to a hyperbola to yield a K_i of 4 mM. Note that the inhibition is competitive, as only the rate of incorporation is reduced while the full amplitude of misincorporation is obtained at all pyrophosphate concentrations.

imply that the chemistry step may be partially rate-determining. Compared with the incorporation of the correct dNTP, where the chemistry step is much faster than the conformational change, the larger elemental effects observed here for the incorrect nucleoside triphosphates would argue for a chemistry step only slightly faster than the conformational change. Nonetheless, since a full elemental effect is not observed, it can be concluded that the conformational change is at least 3–5-fold slower than chemistry.
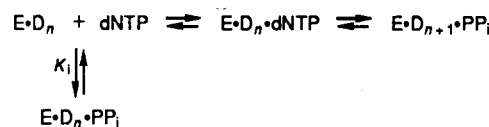
Elementary effect experiments were also carried out for dCTP(αS) at 2 mM and 0.2 mM (data not shown) with the same results, indicating that (1) the α-thio-dNTPs were bound with roughly the same affinities (K_d values) as the oxy-dNTPs and (2) incorrect dNTP binding was not rate-limiting.

Inhibition by Inorganic Pyrophosphate. To address the issue of a possible contribution of pyrophosphorolysis toward fidelity, we monitored the inhibitory effects of pyrophosphate on misincorporation. In a single-turnover experiment with equimolar enzyme and DNA, the time course of misincorporation of dATP into 5'-labeled 25/36-mer was monitored in the presence of increasing concentrations of inorganic pyrophosphate. The results are shown in Figure 4. The addition of 0.5, 2.5, and 5.0 mM pyrophosphate inhibited the rates of misincorporation by factors of 1.1, 1.6, and 2.1, respectively, giving an estimated apparent K_i of 4 mM for pyrophosphate (see inset).

However, regardless of the concentration of pyrophosphate present, the same reaction amplitude was observed. This contrasted with results of an analogous experiment performed with dTTP, the correct nucleoside triphosphate (Patel et al., 1991), where pyrophosphate reduced both the rate of dTTP incorporation (K_i of 2 mM) and the amplitude of incorporation. While the reduction in the rate of incorporation can be thought of as competitive binding between pyrophosphate and substrate dNTP, as shown on the left-hand side of Scheme II, the reduction in the amplitude of incorporation reflects an internal equilibrium driven backward by the addition of pyrophosphate from the right side of the equation. Consequently, the full amplitude attained for misincorporation in the presence of high concentrations of pyrophosphate suggests that the reverse reaction is not kinetically accessible. This implies that pyrophosphorolysis did not remove the misincorporated nucleotide on the time scale of the single turnover.

Pyrophosphorolysis of a Mismatched 3' dNMP. We then sought to determine the rate of pyrophosphorolysis on a ter-

Scheme II

$$E \cdot D_n + dNTP \rightleftharpoons E \cdot D_n \cdot dNTP \rightleftharpoons E \cdot D_{n+1} \cdot PP_i$$

$$K_i \updownarrow$$

$$E \cdot D_n \cdot PP_i$$

minal mismatch by direct measurement. In this experiment, 25/36-mer was enzymatically elongated to 3'-^{32}P-labeled 25A*/36-mer as described under Experimental Procedures. Single-turnover experiments with equimolar enzyme and DNA were carried out in reactions containing inorganic pyrophosphate at concentrations ranging from 0.1 to 20 mM. The time courses of the reactions were monitored by TLC on PEI-cellulose plates, also described under Experimental Procedures. Pyrophosphorolysis was monitored by the appearance of radioactive dATP. For reaction times of up to 30 min, pyrophosphorolysis was not detected (data not shown). On this time scale, a small amount of radioactive dAMP was detected, which could be attributed to the low residual exonuclease activity of the enzyme on mismatched DNA. This rate of excision was known to be in the range of 10^{-5}–10^{-4} s^{-1}. Thus, an upper limit of 10^{-4} can be set for the rate of pyrophosphorolysis of a mismatch at 20 mM pyrophosphate. This, in turn, yields an upper limit for an apparent second-order rate constant, k_{cat}/K_m, of 0.05 M^{-1} s^{-1}. In contrast, the rate of pyrophosphorolysis on a correctly base-paired duplex DNA proceeds at 0.5–2.0 s^{-1} with a K_m of 2 mM, giving a k_{cat}/K_m of $(0.25–1) \times 10^3$ M^{-1} s^{-1} (Patel et al., 1991). Thus pyrophosphorolysis selects against the correctly base-paired primer terminus by a factor of at least 5000.

In a separate experiment, 5'-labeled 25A/36-mer was incubated with exo$^-$ enzyme in the presence and absence of 2 mM pyrophosphate. The reaction was monitored on a denaturing sequencing gel (Figure 5). Without added pyrophosphate, the residual exonuclease removed the terminal mismatch to generate the 25-mer at a rate of 5×10^{-5} s^{-1}. It then paused, unable to excise the next base, which was properly base paired. Discrimination by the residual exonuclease of the mutant enzyme for mismatched base pairs is seen also with the wild-type enzyme (Donlin et al., 1991) but not to the extent seen here with the exo$^-$ mutant. In the reaction containing pyrophosphate, however, a ladder of oligomers $\leq$25 bases long resulted. At first glance this may seem to suggest pyrophosphorolysis; but in actual fact, when the gel slices were quantitated by liquid scintillation counting and the results plotted, it was found that the sum of all the smaller bands in the reaction with pyrophosphate was at all times equal to the total accumulation of the 25-mer in the reaction without pyrophosphate. In other words, the removal of the terminal mismatch occurred at the same rate in both reactions and can therefore be attributed solely to the residual exonuclease activity. Since the product of the initial mismatch excision is a correctly base-paired duplex DNA, a suitable substrate for pyrophosphorolysis, further degradation of the 25-mer in the reaction containing pyrophosphate yielded a ladder of small oligomers.

K_m and k_{off} of a 3'-Mismatched DNA Substrate. In the initial misincorporation experiments with dCTP, the enzyme was observed to polymerize over a mismatch when the next correct dNTP was present. We took advantage of this fact in the following experiment in order to determine the K_m for the mismatched DNA. Increasing concentrations of DNA, ranging from 5 nM to 1 μM of 5'-labeled 25A/36-mer, were reacted with 1 nM enzyme and 200 μM dCTP. The reaction was quenched after various times, and the products were an-

+PP$_i$

0   2.5 5.0 10   15   20   30

-PP$_i$

0   15   30

FIGURE 7: Rate of dissociation of 25A/36-mer from enzyme. Exo⁻ enzyme was preincubated with 25A/36-mer. The reaction was initiated with the addition of an excess of wild-type enzyme. The time course plotted monitors the formation of the excision products. Since the DNA must first dissociate from the exo⁻ enzyme before reassociation with the exo⁺ enzyme, the reaction time course measures directly the rate of the dissociation of the initial enzyme–DNA complex. Final concentrations of reactants were 200 nM exo⁻, 30 nM 25A/36-mer, and 1 μM wild-type enzyme. The data were fitted by using KINSIM with a k_{off} for the 25A/36-mer of 0.3 s⁻¹ and a K_d of 10 nM.
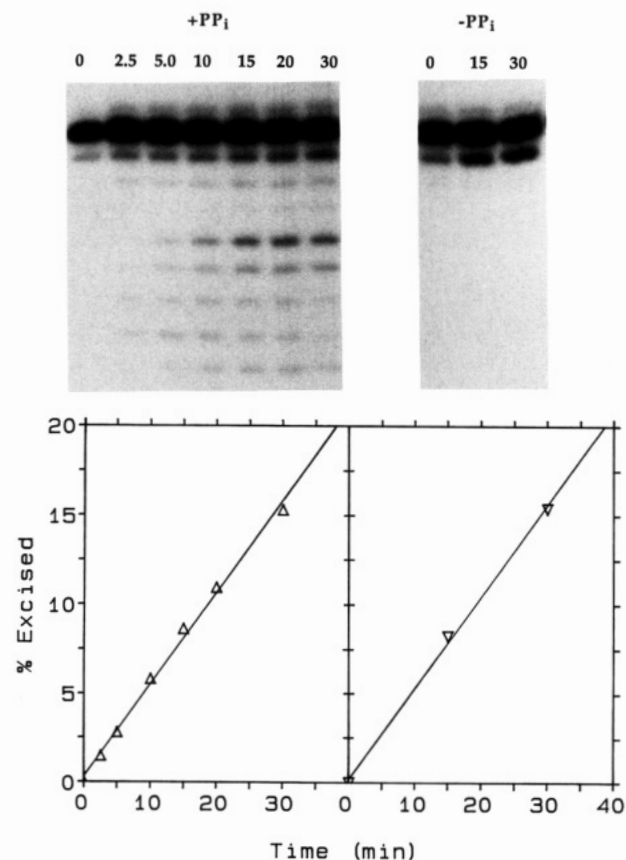
FIGURE 5: Exonuclease versus pyrophosphorolysis. 250 nM 25A/36-mer was incubated with 500 nM enzyme in the presence and absence of 2 mM pyrophosphate. The ladder of smaller oligomers in the reaction with pyrophosphate results from pyrophosphorolysis of *duplex* DNA. The rate of *mismatch* removal is the same with and without pyrophosphate as shown in the plots.

FIGURE 8: K_d of dCTP. K_d determination for the next correct triphosphate, dCTP, on the mismatched DNA 25A/36-mer was performed at 100 nM exo⁻, 300 nM 25A/36-mer, and the indicated concentrations of dCTP. Points were taken at 0, 1, and 5 min, and the initial rates were determined from the slopes of the lines. By 4 mM dCTP (data not shown), severe inhibition of polymerization was observed. Hyperbolic best fit of the rates gave a K_d of 87 μM with a V_{max} of 0.025 s⁻¹.
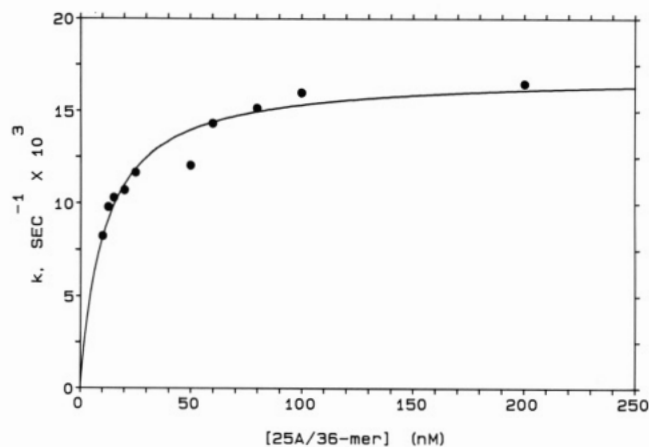
FIGURE 6: K_m of 25A/36-mer. Steady-state K_m determination for the mismatched DNA 25A/36-mer was performed at 5 nM enzyme and 200 μM dCTP at the indicated concentrations of DNA. A hyperbolic fit of the rates gave a K_m of 10 nM.

alyzed on a sequencing gel. The rates of next correct incorporation were measured from initial rates and are plotted as a function of DNA concentration in Figure 6. A hyperbolic fit to the data yielded a K_m for mismatched DNA of 10 nM, which is comparable to the K_d = 18 nM for the correctly base-paired DNA.

To interpret the K_m for the mismatched DNA, it is necessary to know the rate of dissociation of the DNA from the enzyme relative to the rate of reaction. Therefore, we performed the following experiment to measure the rate of dissociation of mismatched DNA from the polymerase site of the enzyme.
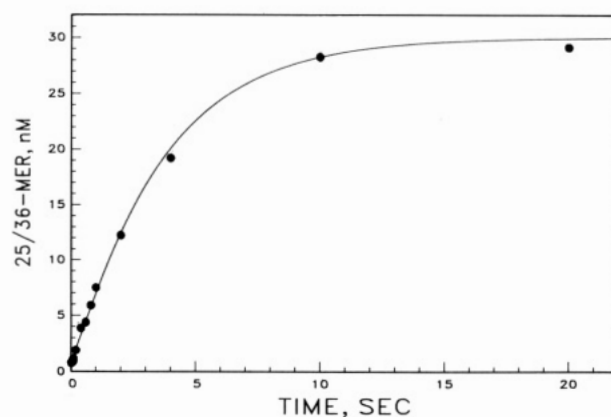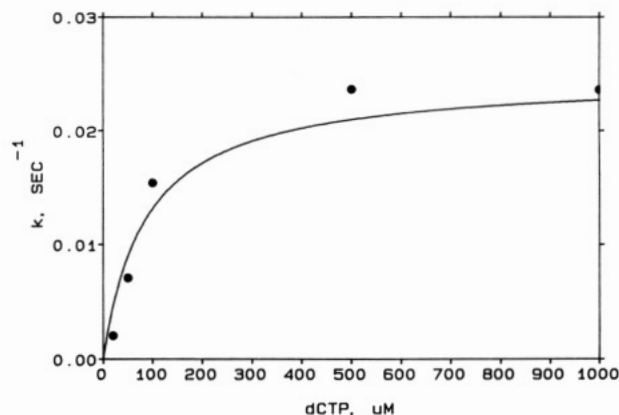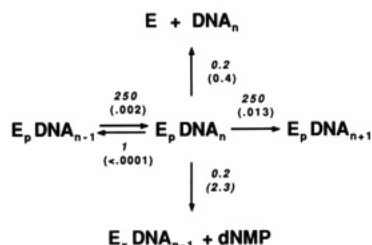
Mismatched DNA (30 nM 25A/36-mer) was preincubated with an excess of exo⁻ enzyme (200 nM) to form an enzyme–DNA complex according to the estimated K_d. The reaction was initiated by the addition of an excess of wild-type enzyme (1 μM). The time course for the excision of the mismatch by the wild-type enzyme is shown in Figure 7. The best fit to the data was obtained by computer simulation at 0.3 s⁻¹. Because the binding of the mismatched DNA into the exonuclease site of the wild-type enzyme and its subsequent excision occur at rates of 5 × 10⁸ M⁻¹ s⁻¹ and 900 s⁻¹, respectively (Donlin et al., 1991), the observed rate of formation of the 25/36-mer is limited by the dissociation of the mismatched DNA from the preformed enzyme–DNA complex, thus providing a direct measurement of the dissociation rate.

K_m, k_{cat}, and Elemental Effect for the Next Correct dNTP. In order to assign the rate-limiting step for incorporation of the next correct dNTP over a mismatch, we determined the kinetic parameters for the next correct nucleoside triphosphate, dCTP. Once again, we used 5′-labeled 25A/36-mer and

Table II: Kinetic Parameters for Correct versus Incorrect Incorporation

parameter	correct[a] K_m (mM)	correct[a] k_{cat} (s⁻¹)	correct[a] k_{obs}[b] (s⁻¹)	incorrect K_m (mM)	incorrect k_{cat} (s⁻¹)	incorrect k_{obs}[b] (s⁻¹)
k_p	0.02	300	250	$\simeq$6–8	$\simeq$0.14	0.002
k_{PP_i}	2	3	1	>20		<0.0001
k_p^{next}	0.02	300	250	0.08	0.025	0.012
k_{off}			0.2			0.4
k_x[c]			0.2			2.8

[a] All parameters for correct dNTP incorporation are from Patel et al. (1991). Excision rates are from Donlin et al. (1991). [b] k_{obs} values for polymerization and pyrophosphorolysis are calculated at estimated physiological concentrations for dNTP of 100 μM and for pyrophosphate of 1 mM, respectively. [c] k_x is the observed rate of excision. The intrinsic rate of excision is very fast (700 s⁻¹). The observed rates cited here are limited by the rate of transfer of the DNA from the polymerase site to the exonuclease site. For correctly base-paired DNA, the transfer rate is limited by the dissociation rate of the DNA from the polymerase site. For mismatched DNA, there is evidence of a direct transfer of DNA to the exonuclease site. All parameters for this process are discussed in detail in Donlin et al. (1991).

Scheme III[a]

$$E + DNA_n$$

$$\big\uparrow \substack{0.2 \\ (0.4)}$$

$$E_pDNA_{n-1} \underset{\substack{1 \\ (<.0001)}}{\overset{\substack{250 \\ (.002)}}{\rightleftarrows}} E_pDNA_n \overset{\substack{250 \\ (.013)}}{\longrightarrow} E_pDNA_{n+1}$$

$$\big\downarrow \substack{0.2 \\ (2.3)}$$

$$E_xDNA_{n-1} + dNMP$$

[a] Kinetic constants given in italics are for correct incorporation. Constants given in parentheses are for misincorporation.

followed the reaction on a denaturing sequencing gel. The concentration dependence of the rate of dCTP incorporation is shown in Figure 8. The best fit of the data to a hyperbola yielded a K_m of 84 μM and a k_{cat} of 0.025 s⁻¹. Unlike the incorporation of the incorrect dNTPs, the incorporation of the next correct dNTP over a mismatch is saturable with respect to the dNTP with a K_m only 4-fold higher than that for dTTP.

We then measured the elemental effect for the next correct incorporation. The experiment was performed under single-turnover conditions with equimolar concentrations of enzyme and 5'-labeled 25A/36-mer. Saturating and subsaturating concentrations of dCTP or dCTP(αS) were used in two separate experiments. In both cases, we observed a large elemental effect of a 60-fold reduction in rate when dCTP(αS) was substituted at the same concentration for dCTP. Figure 9 shows the data at 2 mM dCTP and dCTP(αS). From this we deduce that the chemistry step is largely rate-limiting for correct incorporation over a mismatch.

DISCUSSION

Substrate Discrimination by T7 DNA Polymerase. Table II summarizes the measured kinetic parameters for misincorporation. In Scheme III, we compare these parameters directly with those for correct incorporation as determined in Patel et al. (1991) at estimated physiological concentrations of dNTPs of 100 μM in the context of the kinetic partitioning as described in Scheme I. The rate constants for all steps differ between the two cases, indicating that in general the enzyme is exquisitely sensitive to the "correctness" of the substrates. The most dramatic effects are seen in the remarkable reduction in the rates of polymerization of the incorrect dNTP and of the next correct dNTP over the resultant mismatch as com-
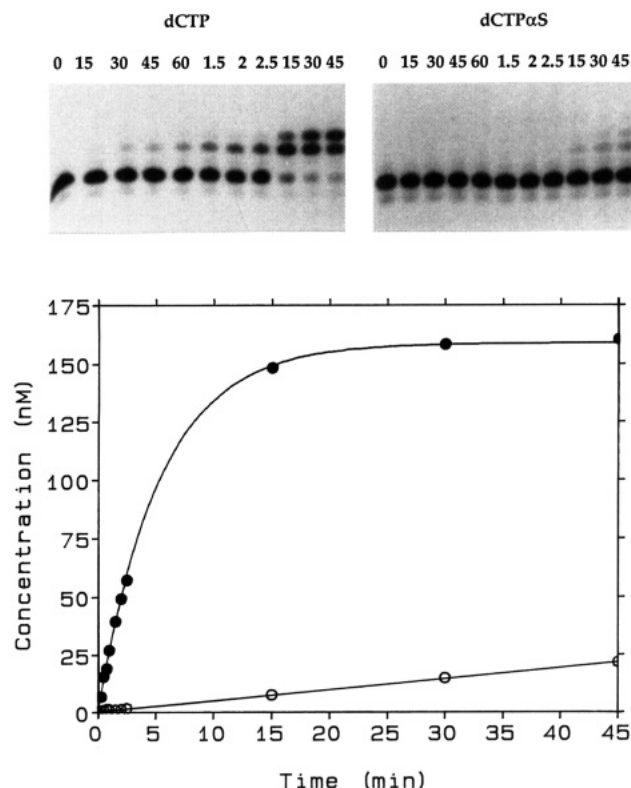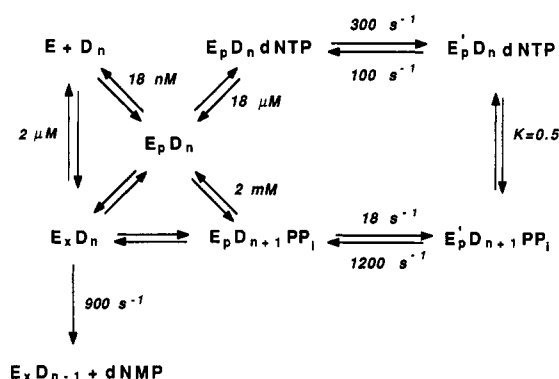

FIGURE 9: Elemental effect for incorporation on mismatched DNA. Time course of misincorporation of dCTP ($\bullet$) at 3.1 × 10⁻³ s⁻¹ and dCTP(αS) (O) at 4.9 × 10⁻⁵ s⁻¹, yielding an elemental effect of 64 for next correct incorporation on a mismatch. Reaction incubations contained 200 nM 25/36-mer, 200 nM enzyme, and 2 mM dCTP or dCTP(αS) under standard reaction buffer conditions.

pared to the rate of correct incorporation. This argues strongly that the replication fidelity is principally driven by substrate discrimination during the polymerization cycle. The wrong dNTPs are recognized as poor substrates and their slow rates of incorporation prevent their addition. In the rare event that a wrong dNTP is added, the resultant mismatched DNA in turn is recognized as a poor substrate, thereby preventing further polymerization over the error. In the former case, no corrective action need be taken; the enzyme releases the wrong dNTP and rebinds the correct one with much greater affinity. In the latter event where the DNA contains a mismatched 3'-end, however, error correction must take place prior to further DNA synthesis. Here, the changes in rate constants are more subtle. The mechanism of error correction involves the kinetic partitioning between the various pathways presented in Scheme III and is discussed in detail by Donlin et al. (1991). In this paper, we are concerned with the mechanism by which the polymerase recognizes and discriminates against the incorrect substrates.

Our approach to this problem of substrate discrimination extends directly from our understanding of the mechanism for correct incorporation. Patel et al. (1991) have shown clearly that, during correct polymerization, a conformational change immediately before chemistry is rate-limiting (Scheme IV). It would therefore seem reasonable to argue that this same conformational change limits the rate of misincorporation.

Our data on misincorporation supports such a model. The observed elemental effects of $\sim$20 were only moderate as compared to an expected full elemental effect of 100; thus chemistry can be eliminated as being solely rate-limiting. Moreover, the lack of a detectable burst during misincorporation places the rate-limiting step for misincorporation before chemistry. Such a burst is observed during the incorporation
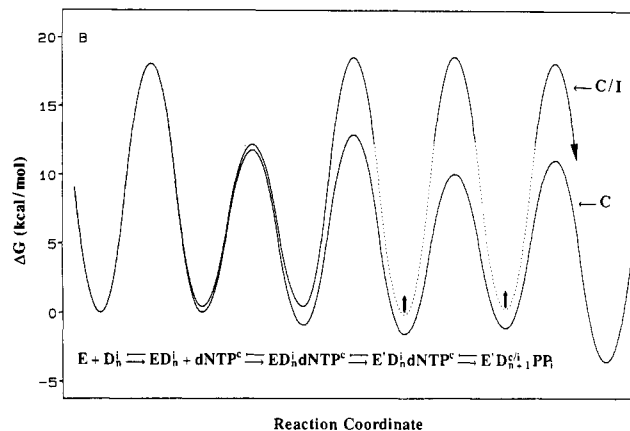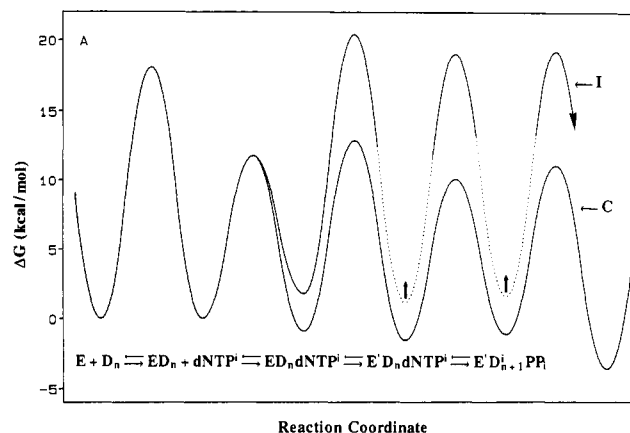
Scheme IV

FIGURE 10: Free energy profiles showing induced-fit discrimination. Dashed lines give the reaction surface for correct incorporation. Free energies are calculated from apparent first-order kinetic constants derived in the Appendix by the equation $\Delta\Delta G = RT[\ln{(\kappa T/h)} - \ln{k_{obs}}]$. A dotted line is used to indicate that the free energies of the internal ground-state species are unknown. However, the mathematical treatment of the elemental effect allows the free energies of the transition states to be calculated (see Appendix); thee are drawn in solid lines. Panel A gives the free energy surface for incorrect dNTP incorporation. Note that the large barrier at extreme left represents the slow off rate of the DNA once bound. For correct incorporation, this large barrier enforces the processivity of DNA synthesis and is therefore the measured steady-state k_{cat}. However, for misincorporation, the highest transition-state barrier occurs at the conformational change step. Panel B shows the reaction surface for the addition of the next correct dNTP over a mismatch.

of a single correct dNTP because the rate of product release, dissociation of the DNA from the enzyme at 0.2 s^{-1}, is slower than the actual rate of dNTP incorporation at 300 s^{-1}. Thus, during the first turnover, 1 equiv of enzyme-bound product is formed at 300 s^{-1} while all subsequent turnovers occur at a steady-state rate of 0.2 s^{-1}.

Since the rates of misincorporation are much slower than 0.2 s^{-1}, the DNA dissociation step is not observed. Nevertheless, if an additional rate-limiting step occurred after chemistry, the kinetics of the first turnover during misincorporation would be biphasic. The faster phase would reflect the rate of formation of the enzyme–product species accumulating immediately before the rate-limiting step. The absence of such biphasic kinetics argues against a rate-limiting step after chemistry. As we discussed in detail in the previous paper (Patel et al., 1991), a single rate-limiting step after chemistry would require severe constraints on the equilibrium constant for the chemistry step such that the amplitude of the fast phase is so diminished as to become undetectable. In particular, the chemistry step would need to be highly unfavorable so that the enzyme-bound product would not accumulate to a sufficient extent even though the rate-limiting step followed chemistry. By our estimate, a chemistry equilibrium constant of less than 0.05 would be necessary to reduce the burst amplitude below detectable limits. In contrast, the chemistry equilibrium for correct incorporation is 0.5 (Patel et al., 1991). We, therefore, favor the simplified model in which the reaction pathway for misincorporation parallels that for correct incorporation, placing the rate-limiting step for misincorporation at a conformational change step immediately before chemistry.

An Induced-Fit Model. In the context of an induced-fit model, the conformational change can be construed as a substrate selection gate. Initial "loose" binding of the correct substrates would trigger a conformational change leading to an active configuration of the enzyme where the key residues in the active site are brought into proper alignment, thereby providing transition-state stabilization for catalysis. This is supported by the rapid (>9000 s^{-1}) rate of the chemistry step following the conformational change. In contrast, binding of the incorrect substrates results in a "bad fit". Consequently, the conformational change occurs at a slower rate and possibly with a less favorable equilibrium constant.

The free energy profiles shown in Figure 10 are constructed on the basis of microscopic rate constants derived from elemental effects as described in the Appendix. These free energy profiles illustrate dramatically the effectiveness of the induced-fit model for substrate discrimination. Furthermore, they demonstrate clearly that selection is effected on the basis of the apparent slow rate of binding of an incorrect substrate in a two-step binding process.

Fersht (1974, 1985) has argued that an induced-fit mechanism cannot contribute any more to selectivity than a simple one-step binding mechanism with the same free energy of binding. However, his analysis was based upon the assumption of a rapid equilibrium binding followed immediately by a rate-limiting chemistry step. Thus, his analysis assumes rate-limiting selectivity in the chemistry step and is therefore somewhat circular. In contrast, as shown in the present case, selectivity by an induced-fit mechanism results when the induced conformational change is rate-limiting.

Interestingly, the binding of either incorrect substrate, incorrect dNTP or mismatched DNA, leads to similar kinetic consequences resulting from the inability of the incorrect substrate to trigger the change in enzyme conformation. It would appear, therefore, that the same induced-fit mechanism is responsible for substrate discrimination in either case. On the surface, this may not seem particularly surprising. However, the fact that the same kinetic step is able to select against either of these substrates permits a glimpse into the topological changes during the induced fit. Presumably initial "loose" binding serves only to collect together the substrates, DNA

and dNTP, bringing them into close proximity in the active site although not in the correct configuration for catalysis. The catalytically active conformation of the enzyme–substrates complex, on the other hand, must have very strict toplogical constraints requiring the substrates to be precisely aligned. Since this conformational change selects for both the correctly base-paired DNA and the correct dNTP, it is tempting to speculate that the topology recognized during the conformational change as being "correct" resembles not that of two distinct substrates but rather that of substrates correctly aligned to resemble the expected product. In other words, the activated conformation would require that the DNA and dNTP can be aligned in such a way as to resemble a fully base-paired duplex DNA template–primer. In this respect, if the DNA contains a 3'-mismatch or if the dNTP does not base pair with the DNA, the resultant "kink" or bulge would impair the conformational change, presumably by the introduction of unfavorable steric interactions within the enzyme cleft. On the other hand, when both DNA and dNTP are aligned correctly, the conformational change takes place smoothly, followed by rapid catalysis. Thus, such a conformational change would afford additional fidelity on topological and steric grounds beyond the thermodynamics of the base-pairing interaction of the substrates.

dNTP Selection—Is It K_m or V_{max}? The question has been raised in the literature as to whether dNTP selection by polymerases is a K_m or a V_{max} phenomenon. Kuchta et. al (1988) has shown that *E. coli* DNA polymerase I shows a strict V_{max} discrimination against incorrect dNTPs, while others have observed strict K_m discrimination in *Drosophila* DNA polymerase α (Boosalis et al., 1987) and *E. coli* Pol III (Sloan et al., 1988). If we were to take these terms literally, we would report that the T7 DNA polymerase shows both K_m and V_{max} discrimination. However, in view of the induced-fit mechanism and changes in the rate-limiting step in the steady state, one must carefully reexamine the meaning of such a distinction.

Because the rate-determining step during processive synthesis is in effect a binding step, and because the rate of the subsequent chemistry step is fast, the steady-state parameters K_m and V_{max} cannot be construed as direct measures of binding versus catalysis in the traditional sense. This is evident in Scheme V, relating the induced-fit mechanism to steady-state parameters k_{cat} and K_m. Since the rate of the reaction would be governed by the apparent second-order rate constant k_{cat}/K_m, the observed rate of the reaction must reflect both K_m and k_{cat}. Conversely, K_m and k_{cat} describe two consequences of the same process—they are both binding parameters for correct incorporation. There exists, therefore, an inherent trap in asking whether dNTP discrimination is a K_m or a V_{max} phenomenon. The answer on a mechanistic level must be that it does not matter. The dichotomy between V_{max} and K_m is purely academic and uninterpretable in the absence of detailed mechanistic information.

Scheme V

$$\text{E}\cdot\text{D}_n + \text{dNTP} \xrightleftharpoons{1/K_m} \text{E}\cdot\text{D}_n\cdot\text{dNTP} \xrightarrow{k_{cat}} \text{E}'\cdot\text{D}_n\cdot\text{dNTP}$$
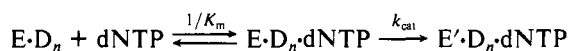
The situations with polymerase α and the α-subunit of Pol III are further complicated by the lack of complete mechanistic descriptions. This makes the appropriate interpretations of steady-state K_m and V_{max} values practically impossible. The processivity of any polymerase is enforced by the slow rate of DNA release. In experiments designed to examine a single-nucleotide incorporation or polymerization over short stretches of DNA less than the processive length, steady-state turnover is limited by the slow DNA dissociation rate. In other words,

steady-state V_{max} gives the rate of dissociation of the DNA from enzyme. Furthermore, one should be extremely cautious of mechanistic studies of polymerases in the absence of a full complement of accessory proteins. In the present case, the binding of the accessory protein, thioredoxin, produces marked changes in the binding of the polymerase to the DNA, in the kinetics of incorporation, and in the rate of misincorporation (unpublished observations); and so, studies of polymerases in the absence of accessory proteins may have little physiological significance.

Neither polymerase α nor the α-subunit of Pol III by itself is thought to be highly processive; even so, they are far from being purely distributive (processivity of 1). It has been estimated that polymerase α, for example, has a processivity of 200 (Challberg & Kelly, 1989), which to a first approximation would give a 200-fold difference between the rate of polymerization and the off rate. The measured steady-state V_{max}, therefore, must still be limited by the DNA off rate. Interestingly, Boosalis et al. (1987) reports a V_{max} for polymerase α of 2.2 s^{-1}, which seems much too slow for a polymerization rate but falls, rather, in the expected range for a DNA dissociation rate. Furthermore, if 2.2 s^{-1} were the DNA off rate, the processivity of 200 would give an estimated true polymerization rate of 400–500 s^{-1}.

This results in a serious problem for any fidelity studies performed under steady-state conditions because the rate of misincorporation is likely to be slower than the off rate, especially at subsaturating concentrations of dNTPs. Hence, the V_{max} measured for misincorporation gives the rate of a different step in the kinetic pathway. As a result, the values of V_{max} determined for correct and incorrect dNTPs cannot be compared directly since they measure the rates of different processes. Nor does the use of "relative velocities" (Boosalis et al., 1987) circumvent this problem, because the problem does not lie in the manipulation of data but stems from the basic limitation inherent in the steady-state design of the experiment. The induced-fit model for discrimination we propose does not rely on any interpretations of K_m and V_{max}. Indeed, it is precisely because we have first elucidated all the elementary steps in the kinetic pathway by pre-steady-state methods that we can confidently determine that the steady-state K_m and V_{max} are binding parameters.

The situation with Pol I, however, is more puzzling. There, the elementary kinetic pathway has been studied by using pre-steady-state techniques (Kuchta et al., 1987, 1988). The model proposed for fidelity on the basis of these studies, however, deviates significantly from the one we present here for T7 polymerase in two respects. First, the rate of misincorporation by Pol I is saturable at concentrations of the incorrect dNTPs within an order of magnitude of the correct ones. Second, in their mechanism for the incorporation of an incorrect dNTP in Pol I, the rate-limiting step is proposed to occur after chemistry, whereas it occurs before chemistry for correct incorporation.

The fact that Pol I shows little or no discrimination between correct and incorrect dNTPs on initial binding can perhaps be reconciled by the fact that Pol I is a repair enzyme with low processivity. Since the wrong dNTPs with their comparably low K_m values would act as competitive inhibitors of correct incorporation, such a lack of discrimination would result in lowered efficiency of DNA synthesis. While such a kinetic disadvantage might be tolerated in a repair enzyme, it would be detrimental for a true replication enzyme like T7. Perhaps, on the basis of these results, the view of Pol I as a prototype enzyme for studies on the mechanism of DNA po-

lymerization should be seriously reexamined.

The change in rate-limiting step is very much more difficult to rationalize from a purely mechanistic point of view, especially since no kinetic evidence exists for the same rate-limiting step following correct incorporation. In their study, the inclusion of such a step in the misincorporation scheme was necessitated by the observation of biphasic kinetics in the pre-steady-state addition of an incorrect dNTP and the failure to accumulate certain incorrect products. However, these curious results are severely compromised by the fact that the experiments were performed with an exo$^+$ polymerase. Consequently, the biphasic nature of the reaction time course could be interpreted to reflect instead an approach to some steady-state balance between the rates for forward misincorporation and mismatch excision. Indeed, in subsequent experiments performed with an exo$^-$ enzyme, misincorporation does proceed to full amplitude (Eger et al., 1990). The lower than expected accumulation of mismatches during steady-state turnover may be due to a preferential binding and excision of mismatches by the exonuclease, as observed by Donlin et al. (1991).

DNA Selection and Kinetic Partitioning. In the rare event of misincorporating an incorrect dNTP, the enzyme must select against the resultant mismatched DNA. Recalling Scheme III, there exist four possible pathways out of the E·D$^i_{n+1}$ complex: (1) direct removal of the error via the microscopic reversal of the polymerization reaction—pyrophosphorolysis, (2) polymerization over the error, (3) dissociation from the mismatched DNA, and (4) transfer of the mismatched DNA directly into the exonuclease site for repair.

The first of the four options, the involvement of pyrophosphorolysis and pyrophosphate exchange in fidelity, has long been proposed in the literature (Brutlag & Kornberg, 1972; Deutscher & Kornberg, 1969; Hopfield, 1976; Ninio, 1975), sometimes referred to as kinetic proofreading models of fidelity. It is, however, worth noting that the original models were proposed as purely mathematical constructs. There has not been any direct evidence in the literature in support of the role of pyrophosphorolysis in mismatch repair or prevention other than the observation that polymerization is less accurate at high pyrophosphate concentrations (Kunkel et al., 1986). We present here direct and conclusive evidence that pyrophosphorolysis of a mismatch, with $k_{cat}/K_m < 5 \times 10^{-2}$ M^{-1} s^{-1}, is not a kinetically viable pathway. Therefore, the decrease in fidelity induced by pyrophosphate can be explained by the selective pyrophosphorolysis of correctly base-paired products. This selectivity can be understood in the context of the induced-fit mechanism, where the polymerase selects against the mismatched DNA and makes the chemistry step inaccessible to pyrophosphate.

The induced-fit selection against polymerization over a mismatched 3'-end has already been discussed and is shown diagrammatically in Figure 10B. Correct incorporation over a mismatch is a highly undesirable process whereby the actual misincorporation would become effectively sealed in. The k_{cat} (0.025 s^{-1}) and K_m (87 μM) for this process allow calculation of the rate at physiological concentrations of dNTP (100 μM) to give an estimate of 0.012 s^{-1}. It can be seen that the induced-fit mechanism very effectively selects against incorporation over mismatches as it occurs 2×10^4-fold slower than for normal polymerization, causing the enzyme to "stall" after the misincorporation.

During this stall time, kinetic partitioning takes place. The remaining two possible kinetic pathways, dissociation of the enzyme–DNA complex and the direct channeling of mis-

Table III: Fidelity of T7 DNA Polymerase^a

ϕ_p	$\dfrac{(k_{cat}/K_m)_c + (k_{cat}/K_m)_i}{(k_{cat}/K_m)_i}$	$(0.15–3.8) \times 10^6$
ϕ_x^b	$\dfrac{k_p^{c/i} + 0.5k_{off} + k_{p \to x}}{k_p^{c/i}}$	210
Φ	$\phi_p\phi_x$	$(0.38–9.4) \times 10^8$

^{a}The contributions toward fidelity by polymerase, ϕ_p, and exonuclease, ϕ_x are defined as described in the text. ^{b}The derivation of ϕ_x is detailed in the accompanying manuscript (Donlin et al., 1991).

matched DNA into the exonuclease site for editing, with respect rates of 0.4 s^{-1} and 2.8 s^{-1}, would compete effectively with forward polymerization. A detailed analysis of this kinetic partitioning mechanism is presented in the following paper in this series (Donlin et al., 1991). It suffices to note here that this kinetic partitioning is driven to a significant extent by the stalling as a result of induced-fit discrimination against the mismatched DNA.

Calculation of the Fidelity Parameter Φ. Finally, we can calculate a net fidelity parameter Φ to be the product of ϕ_p and ϕ_x, representing components of fidelity contributed by the polymerase and the exonuclease, respectively. In general, fidelity is defined as the reciprocal of the error frequency. The error frequency is defined as the sum of the rates of all those pathways leading to the formation of the incorrect product divided by the sum of the rates of all pathways leading to the formation of the correct and the incorrect products.

For dNTP discrimination, the situation is simple since the binding and incorporation of the incorrect and the correct substrates are competitive. Hence, the selectivity factor is simply the ratio of the k_{cat}/K_m values. The component contributed by the polymerase to net fidelity is therefore defined

$$\phi_p = \frac{(k_{cat}/K_m)_c + (k_{cat}/K_m)_i}{(k_{cat}/K_m)_i} = 7.5 \times 10^5$$

Because pyrophosphorolysis does not occur on a mismatch, the exonuclease must be called upon to correct a mistake. The fidelity contributed by this process is driven by the slow rate of polymerization over the mismatch in comparison to the relatively rapid rate of partitioning into the exonuclease site for repair. Consequently, a $\phi_x = 210$ can be calculated. The actual partitioning functions involved in this derivation are presented in detail in Donlin et al. (1991).

In their treatment of the polymerase α from calf thymus, Perrino and Loeb (1989) introduce the term "relative extension frequency", defined as the rate of polymerization over a mismatch relative to the rate of normal polymerization. It must be stressed that, in terms of fidelity, this term cannot be meaningful. The stalling after misincorporation provides an excess of time during which editing can occur. Since correct polymerization cannot occur until after the mismatch has been removed, the calculation of fidelity must be restricted to only those pathways that directly affect editing.

The overall fidelity Φ can be calculated as the product of ϕ_p and ϕ_x. For T7 DNA polymerase, Φ is in the range of $(0.4–9.4) \times 10^8$ (Table III). Boosalis et al. (1988) report a value for the error frequency of polymerase α from *Drosophila* of 2.1×10^{-4}, corresponding to a fidelity parameter of 4.8×10^3. This surprisingly low number can perhaps in part be rationalized by the lack of editing. It may be that an as yet unidentified exonucleolytic subunit would play a physiological role in editing. Even so, the value of 4.8×10^3 is significantly lower than the ϕ_p, the polymerase component of fidelity, of
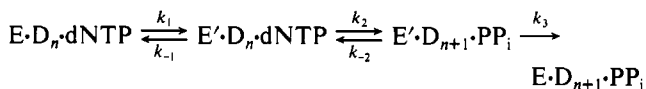
7.5×10^5 reported here for T7 DNA polymerase. We feel that this discrepancy may reflect the V_{max} of 2.2 s^{-1} in those studies as being too slow to represent the true rate of DNA synthesis. If the estimated rate of 400 s^{-1} (see above discussion on the processivity of polymerase α) is substituted for the rate of correct incorporation, a correspondingly higher fidelity of 8.7×10^5 can be extrapolated. The validity of this hypothesis could be unequivocally established by the performance of one single-turnover experiment.

DNA Sequence Dependence. We have performed all our experiments with the 25/36-mer as the basic DNA template–primer system. This may appear at first sight to ignore the question of base and sequence dependence. This is not so. Indeed, we have chosen to restrict our study to the 25/36-mer for the explicit purpose of excluding base- and sequence-dependent effects in order to derive a complete mechanism by using a single substrate DNA. The question of base and sequence dependence by itself is an interesting problem, and efforts are currently under way to address this issue systematically. In this current study, however, we have purposely eliminated that additional variable by using only the 25/36-mer so that the kinetic scheme solved for misincorporation can be directly compared with the scheme of the normal polymerization cycle. While on the one hand we acknowledge that the actual rates of misincorporation and/or correct incorporation over a mismatch will vary with DNA sequence, preliminary data from our sequence-dependence studies indicate that the three k_{cat}/K_m values determined in the present study encompass the full range of k_{cat}/K_m values determined for many different DNA sequences. Consequently, sequence-dependent variations in selectivity, being in the range of one order of magnitude (Petruska & Goodman, 1984) are insignificant in comparison to the many orders of magnitude effects we have described in this study.

Conclusion. In conclusion, we have characterized the steps in the kinetic pathway responsible for the prevention and detection of errors in the polymerization cycle of T7 DNA polymerase. We propose that an induced-fit binding mechanism selects very efficiently for the binding of the correct dNTP, with a net contribution toward fidelity, ϕ_p, of 10^5–10^6 (Table III). In the rare event of misincorporation, the resultant mismatched DNA causes the enzyme to stall. The selectivity against incorrect DNA, calculated as the kinetic partitioning of the mismatched DNA between forward polymerization and exonucleolytic repair, contributes an additional factor, ϕ_x, of 2.1×10^2. Together, a net fidelity parameter Φ of 10^7–10^9 is derived, which is sufficient to account for the high degree of fidelity as estimated in vivo.

APPENDIX

Kinetic Analysis and Derivation of Rate Constants from Elemental Effects. In the reaction scheme

$$E{\cdot}D_n{\cdot}dNTP \underset{k_{-1}}{\overset{k_1}{\rightleftharpoons}} E'{\cdot}D_n{\cdot}dNTP \underset{k_{-2}}{\overset{k_2}{\rightleftharpoons}} E'{\cdot}D_{n+1}{\cdot}PP_i \overset{k_3}{\longrightarrow}$$
$$E{\cdot}D_{n+1}{\cdot}PP_i$$

the net forward rate of product formation, k_f, is given by

$$k_f = \frac{k_1 k_2 k_3}{k_1 k_{-2} + k_1 k_3 + k_{-1} k_{-2} + k_{-1} k_3 + k_2 k_3} \quad (1a)$$

$$k_1 k_2 k_3 = k_f(k_1 k_{-2} + k_1 k_3 + k_{-1} k_{-2} + k_{-1} k_3 + k_2 k_3) \quad (1b)$$

Assuming a full elemental effect of a 100-fold reduction in the forward and reverse rates of the chemistry step (Gupta et al., 1984), given by k_2 and k_{-2} for the incorporation of a dNTP(αS), the observed net forward rate of dNTP(αS) incorporation, $k_f^{\alpha S}$, is given by

$$k_f^{\alpha S} = \frac{k_1 k_2 k_3}{k_1 k_{-2} + 100 k_1 k_3 + k_{-1} k_{-2} + 100 k_{-1} k_3 + k_2 k_3} \quad (2a)$$

$$k_1 k_2 k_3 = k_f^{\alpha S}(k_1 k_{-2} + 100 k_1 k_3 + k_{-1} k_{-2} + 100 k_{-1} k_3 + k_2 k_3) \quad (2b)$$

$$k_1 k_2 k_3 = \frac{k_f}{E_{obs}}(k_1 k_{-2} + 100 k_1 k_3 + k_{-1} k_{-2} + 100 k_{-1} k_3 + k_2 k_3) \quad (2c)$$

where E_{obs} is the observed net elemental effect, defined as $k_f/k_f^{\alpha S}$.

Setting (1b) equal to (2c) and rearranging yields

$$k_2 = \frac{k_1 k_3 (K_1 + 1)(100 - E_{obs})}{(E_{obs} - 1)\left(k_1 \dfrac{K_1 + 1}{K_2} + k_3 K_1\right)} \quad (3)$$

where the microscopic equilibrium constants K_1 and K_2 are defined as k_1/k_{-1} and k_2/k_{-2}, respectively. Alternatively, k_2 can be derived directly from eq 1b:

$$k_2 = \frac{k_f k_1 k_3 \left(1 + \dfrac{1}{K_1}\right)}{k_1 k_3 = \dfrac{1}{K_2} k_1 k_f - \dfrac{1}{K_1 K_2} k_1 k_f - k_f k_3} \quad (4)$$

Setting (3) equal to (4) yields

$$k_1 = \frac{k_3}{k_3 \dfrac{100 - E_{obs}}{99 k_f} - \dfrac{K_1 + 1}{K_1 K_2}} \quad (5a)$$

$$K_1 = \frac{k_3 \dfrac{99 k_f}{100 - E_{obs}}}{k_3 - \dfrac{99 k_f}{100 - E_{obs}} \Lambda_2} \quad (5b)$$

From eq 5b, mathematical lower limits for k_1 and k_3 are defined directly by the hyperbolic asymptotes:

$$k_1 > \frac{99 k_f}{100 - E_{obs}} \qquad k_3 > \frac{99 k_f}{100 - E_{obs}} \Lambda_2 \qquad \Lambda_2 = \frac{K_1 + 1}{K_1 K_2}$$

Substitution of (5a) back into (3) yields

$$k_2 = k_f \Lambda_1 \frac{100 - 1}{E_{obs} - 1} \qquad \Lambda_1 = \frac{K_1 + 1}{K_1} \quad (6)$$

Equation 6 thus explicitly defines the forward rate of the internal chemistry step.

To derive the *microscopic* forward rate constants describing the change in free energy from each discrete ground state to the following transition state requires knowledge of K_1 and K_2. This is because K_1 and K_2 directly relate the free energies of the three ground state species. Unfortunately, because the reverse reaction cannot be measured, these internal equilibria likewise cannot be measured. Hence, the free energies of internal ground-state species are inaccessible.

This limitation, however, does not apply to the calculation of the transition-state free energies given by $\Delta G^\ddagger$. This is because K_1 and K_2 appear only in the terms of Λ_1 and Λ_2. The mathematical context of these terms in eqs 5 and 6 is such that they approximate "normalization" functions for the microscopic rate constants k_2 and k_3 with respect to the free energy of the initial ground-state species, E·D$_n$·dNTP. This is reflected in the fact that Λ_1, which corresponds to the normalization factor for k_2, is dependent only on K_1 while Λ_2, which corresponds to the normalization factor for k_3, is dependent on both K_1 and K_2. As a result, the overall differences

between the two transition-state free energies, $\Delta G^{\ddagger}$, corresponding to k_2 and k_3 are relatively insensitive to differences in the assumed values for K_1 and K_2. Consequently, the uncertainty in the free energy surface can be restricted to the ground-state free energies of the various enzyme-bound intermediates.

In constructing the free energy diagrams shown in Figure 10, we make the assumption that the equilibrium constants for the internal ground states are approximated by the analogous constants describing correct incorporation. Thus, the equilibrium constants, K_1 for the conformational change step and K_2 for the chemistry step, are arbitrarily fixed at 3 and 0.5, respectively (Patel et al., 1991). This clearly represents a lower limit on the ground-state free energy of the intermediate species, yielding therefore lower limits for the microscopic forward rate constants k_2 and k_3. Alternatively, upper limits for the intermediate ground-state energetics can be estimated by setting the reverse microscopic rates k_{-1} and k_{-2} equal to the analogous rate constants for correct incorporation of 100 and 26 400 s^{-1}, respectively.

For misincorporation with a k_{cat} of 0.14 s^{-1} for an estimated K_m of 7 mM and an overall elemental effect of 20, a chemistry rate, k_2, of 0.98 s^{-1} can be calculated from eq 6. Likewise, eq 5b gives the mathematical asymptotic limit for k_1 of 0.17 s^{-1} at infinitely fast k_3. However, since the mathematical model allows the rate-limiting step to be before or after chemistry, k_1 must be further constrained to prevent k_2 from being rate-limiting. For this limit, we choose k_3 to be 10 times the observed k_f. Accordingly, an upper limit for k_1 of 0.26 s^{-1} can be calculated. This upper limit is used in the construction of the energy diagrams shown in Figure 10. Similarly, for the next correct incorporation with a k_{cat} of 0.025 s^{-1} and an overall elemental effect of 60, k_2 is calculated to be 0.056 s^{-1} with k_1 bounded between 0.062 and 0.182 s^{-1}.

The more serious caveat to the above treatment stems from the naïve assumptions made concerning interpretations of the elemental effect. While on the one hand the literature routinely assumes that thio substitution affects only the rate of chemistry at the substituted phosphate center, numerous investigators have noted evidence to the contrary. Thus, Mizrahi et al. (1985) and Kuchta et al. (1987) have noted that the observed elemental effect in the forward and the reverse—i.e., pyrophosphorolysis—direction for *E. coli* DNA polymerase I differ by at least an order of magnitude. Perhaps even more disturbing is the observation that phosphorothioate diester bonds in the DNA backbone alter the DNA's secondary structure (Eckstein & Jovin, 1983), and can therefore alter the protein–DNA binding interactions. Consequently, the above treatment cannot be regarded as a rigorous, quantitative analysis. Rather, it has been intended only as an approximate means to probe the free energy surface of polymerization.

Registry No. dATP, 1927-31-7; dCTP, 2056-98-6; dGTP, 2564-35-4; dATP(αS), 64145-28-4; dCTP(αS), 64145-29-5; dGTP(αS),

82337-56-2; DNA polymerase, 9012-90-2; pyrophosphate, 14000-31-8.

REFERENCES

Bernad, A., Blanco, L., Lázaro, J. M., Martin, G., & Salas, M. (1989) *Cell 59*, 219–222.

Boosalis, M. S., Petruska, J., & Goodman, M. F. (1987) *J. Biol. Chem. 262*, (30), 14689.

Brutlag, D., & Kornberg, A. (1972) *J. Biol. Chem. 247*, 241.

Challberg, M. D., & Kelly, T. J. (1989) *Annu. Rev. Biochem. 58*, 671.

Deutscher, M. P., & Kornberg, A. (1969) *J. Biol. Chem. 244*, 3019.

Donlin, M. J., Patel, S. S., & Johnson, K. A. (1991) *Biochemistry* (third of three papers in this issue).

Eckstein, F., & Jovin, T. M. (1983) *Biochemistry 22*, 4546.

Eger, T. E., Kuchta, R. D., Carroll, S. S., Benkovic, P. A., Dahlberg, M. E., Joyce, C. M., & Benkovic, S. J. (1990) *Biochemistry* (submitted for publication).

Fersht, A. (1974) *Proc. R. Soc. London, Ser. B. 187*, 397.

Fersht, A. (1985) *Enzyme Structure and Mechanism*, 2nd ed., p 363ff, W. H. Freeman & Co., New York.

Gupta, A. P., Benkovic, P. A., & Benkovic, S. J. (1984) *Nucleic Acids Res. 12*, 5897.

Herschlag, D. (1987) *Bioorg. Chem. 16*, 62.

Hopfield, J. J. (1974) *Proc. Natl. Acad. Sci. U.S.A. 71*, 4135.

Kuchta, R. D., Mizrahi, V., Benkovic, P. A., Johnson, K. A., & Benkovic, S. J. (1987) *Biochemistry 26*, 8410.

Kuchta, R. D., Benkovic, P. A., & Benkovic, S. J. (1988) *Biochemistry 27*, 6716.

Kunkel, T. A., Beckman, R. A., & Loeb, L. A. (1986) *J. Biol. Chem. 261*, 13610.

Loeb, L. A., & Kunkel, T. A. (1982) *Annu. Rev. Biochem. 52*, 429.

Mizrahi, V., Henrie, R. N., Marlier, J. F., Johnson, K. A., & Benkovic, S. J. (1985) *Biochemistry 24*, 4010.

Ninio, J. (1975) *Biochimie, 57*, 587.

Page, M. I. (1986) in *Accuracy in Molecular Processes* (Kirkwood, T. B. L., Rosenberger, R. F., & Galas, D. J., Eds.) p 37, Chapman and Hall, London.

Patel, S. S., Wong, I., & Johnson, K. A. (1991) *Biochemistry* (first of three papers in this issue).

Perrino, F. W., & Loeb, L. A. (1988) *J. Biol. Chem. 264*, 2898.

Petruska, J., & Goodman, M. F. (1984) *J. Biol. Chem. 260*, 7533.

Reha-Krantz, L. J. (1988a) in *DNA Replication and Mutagenesis* (Moses, R. E., & Summers, W. C., Eds.) p 34, American Society for Microbiology, Washington, D.C.

Reha-Krantz, L. J. (1988b) *J. Mol. Biol. 202*, 711.

Tabor, S., & Richardson, C. C. (1985) *Proc. Natl. Acad. Sci. U.S.A. 82*, 1074.

Tabor, S., & Richardson, C. C. (1987) *J. Biol. Chem. 262* (33), 16212.